Research Article

Minru Liu, Zhihua Tang, Zhenrong Lin, Huafang Guo, Zhen Yu*, Xiaoming Liu, Kejing Fang

Insight into the cadmium and zinc binding potential of humic acids derived from composts by EEM spectra combined with PARAFAC analysis

https://doi.org/10.1515/chem-2020-0005
received April 4, 2019; accepted November 10, 2019.

Abstract: To investigate the characteristics of humic acids (HAs) and the combined effects of HAs on heavy metals, three HAs derived from kitchen waste compost (KW), pig manure compost (PM), and green waste compost (GW) were exposed to Cd(II) and Zn(II). The elemental contents and functional groups of HAs were different due to different raw materials. Fulvic-, humic-like content C1, humic-like content C4, and two protein-like contents C2 and C3 were identified in three HAs by EEM-PARAFAC analysis. The effects of HAs on heavy metals were associated with the metal species and HA source. Our results reveal that titrating Cd(II) caused stronger fluorescence quenching compared to titrating Zn(II) for all HAs. C1 and C4 of KW-HAs and PM-HAs showed fluorescence quenching after Cd(II) was added, whereas negligible fluorescence quenching was found when Zn(II) was added. In addition, C1 and C4 in the GW-HAs did not show obvious fluorescence quenching regardless of whether Cd(II) or Zn(II) was added. C3 in all HAs caused significant fluorescence quenching, suggesting that C3 plays an important role affecting the mobility of heavy metals. Consequently, these results suggest that HAs from KW and PM have greater potential for Cd-contaminated soil remediation than those from GW.

***Corresponding author: Zhen Yu,** Guangdong Key Laboratory of Integrated Agro-environmental Pollution Control and Management, Guangdong Institute of Eco-environmental Science & Technology, Guangzhou 510650, China, E-mail: yuzhen@soil.gd.cn
Minru Liu, Zhihua Tang, Zhenrong Lin, Huafang Guo, Kejing Fang, Guangdong Provincial Key Laboratory of New and Renewable Energy Research and Development, Guangzhou Institute of Energy Conversion, Chinese Academy of Sciences, Guangzhou 510640, China
Xiaoming Liu, Guangdong Key Laboratory of Integrated Agro-environmental Pollution Control and Management, Guangdong Institute of Eco-environmental Science & Technology, Guangzhou 510650, China

Keywords: heavy metal, humic-like substance, protein-like substance, binding parameter, EEM-PARAFAC analysis.

1 Introduction

Vast amounts of organic solid wastes, such as kitchen waste, pig manure, and green waste, are generated in China and continue to increase annually [1-3]. Utilization of these wastes in an environmentally friendly manner has received much attention [4-6]. Composting is an effective and acceptable biological process to convert organic solid wastes into fertilizer or soil conditioner for agricultural use, as composting improves soil fertility, reduces greenhouse gas emissions, and remediates soil heavy metal pollution [7-11]. During composting, unstable organic solid wastes are transformed into stable complex compounds such as humic acids (HAs) [12,13], which have larger molecular weights and higher aromaticity [14]. Until now, the structural information of many HAs such as aromatic derivatives, phenolic fragments, substituted benzoic acids, quinones, carbohydrates, fatty acids, and peptides has been described by researchers [15]. As many of the functional groups carried on HAs interact with heavy metals [16], it might be feasible to use HAs to affect the mobilization behaviour of heavy metals. However, the compositions of HAs differ because they are formed from different raw materials [17], so it is necessary to compare the binding capacity of different HAs to heavy metals.

Fluorescence excitation-emission matrix (EEM) spectroscopy has been used to investigate the binding capacity between HAs and heavy metals due to its relatively low-cost, simple instrumentation, low sample volume, and high sensitivity [18,19]. In addition, EEM spectra combined with the PARAFAC mathematical model have been used to provide individual groups of fluorescent components [20]. This method reduces the EEM dataset into a set of trilinear terms and a residual

array and identifies how many fluorescent components is appropriate to decompose by a split half analysis, residual analysis, and visual inspection [21]. Many studies have used this method to quantitatively assess the binding degree between complex organic compounds and heavy metals. Wu et al. [22] compared the fluorescent characteristics between Cu(II), Cd(II) and individual molecular weight fractions of dissolved organic matter (DOM) in landfill leachate by EEM-PARAFAC. He et al. [23] also described the characteristics of humic substances from compost and their binding properties with heavy metals using this method.

All HAs, DOM, and water-extractable organic matter (WEOM) can bind with heavy metals [24-26]. However, many studies have only focused on complexation between DOM or WEOM and heavy metals, particularly Cu**(II)**. For example, Yuan et al. [24] reported that DOM derived from decomposing macrophytes shows an obvious quenching effect by Cu**(II)**. He et al. [25] investigated the binding capacities of WEOM from composted municipal solid wastes on Cu**(II)**, and suggested that the composting treatment increased the Cu**(II)** binding capacities. The binding behaviour between HAs and heavy metals, particularly metals besides Cu**(II)**, has not been investigated sufficiently. As Cd**(II)** and Zn**(II)** pollution in soil is very serious, particularly around the lead-zinc mines in China [27,28], using huge amounts of compost products from kitchen waste, pig manure, and green waste is a potential solution to repair Cd- and Zn-contaminated soils. Therefore, an assessment of binding capacities between HAs derived from composts and Cd**(II)** and Zn(II) is necessary to help us understand the binding mechanisms between them.

The objectives of this study were to: (1) characterize the structure and composition of HAs derived from KW, PM, and GW; (2) compare the binding capacities of HAs from different composts with Cd**(II)** and Zn**(II)**; and (3) investigate the binding behaviour using the stability constant (log K_m). This study will offer theoretical support for using composts to repair Cd- and Zn-contaminated soils.

2 Materials and methods

2.1 Sample collection and storage

Three compost samples (KW, PM, and GW) were collected from different full-scale composting plants, located in Guangdong Province, China. Three portions were taken from each sample after sampling. The first portion was used to determine moisture content and pH. The second portion was air-dried to determine organic matter and total N. The third portion was stored at 4°C before extracting the HAs. Details of the sample properties are described in Table 1.

Table 1: Properties of the compost samples.

Parameter	KW	PM	GW
Moisture (%)	30.2±0.27	23.6±0.31	28.6±0.20
pH	7.38±0.09	7.5±0.07	7.42±0.10
Total N (g kg^{-1})	34.3±0.25	38.8±0.19	15.4±0.29
Organic matter (%)	54.17±0.35	69±0.52	45.1±0.24

2.2 Extraction of HAs

HAs were extracted according to the method described by Zhang et al. [29]. Briefly, one of the three compost samples (100 g) was mixed with 150 mL of 2% HF. The mixture was shaken for 16 h at a rotational speed of 180 rpm and room temperature and then centrifuged at 8,000 rpm for 6 min. The precipitate was used to repeat the above procedure three times after removing the supernatant each time. Then, 150 mL of 0.1 M NaOH was mixed with the precipitate and shaken for 24 h at a rotational speed of 180 rpm and room temperature. The supernatant was separated from the residue by centrifugation at 8,000 rpm for 6 min. This procedure was repeated three times, and all of the supernatants were pooled together. The extracted HAs were obtained by adding 2 M HCl (24 h at room temperature, pH < 2) to the supernatant. The HAs were repeatedly washed with deionized water and freeze-dried for future research.

2.3 Binding experiments

Batch tests were carried out to obtain the quenching performance of the KW, PM, GW-derived HAs on Cd**(II)** and Zn**(II)**, and to compare the different binding capacities. Freeze-dried HAs were dissolved in 1.0 M KOH individually for the Cd**(II)** quenching titration. After adjusting the pH to 7.0 ± 0.1 with 1.0 M HCl, the organic carbon content in the HA samples was 12.5 mg/L. A 25 mL aliquot of

the HAs was carefully transferred to a 50 mL volumetric flask, and 0, 12.5, 25, 50, 75, 100, 125, 150, 175, 200, 225, or 250 µL $CdCl_2$ was added (0.01 µmol/L pH = 7.0 ± 0.1) to each volumetric flask to be certain that the Cd(II) final concentrations ranged from 0 to 100 µmol/L. In addition, $ZnCl_2$ was prepared for the Zn(II) quenching titration. The same procedure was followed except that the pH values of the HAs and $ZnCl_2$ were adjusted to 6.0 ± 0.1. The solutions were mixed for 24 h in an oscillator at room temperature before EEM spectral scanning.

2.4 HAs characterization

An elemental analysis including C, H, N, O, and S of the freeze-dried HAs was carried out with a Vario EL cube elemental analyser. The atomic ratios which refer to the molar ratios of the elements were computed by dividing the content of elements in percentage obtained from the analysis by their atomic mass [30]. Fourier transform-infrared (FTIR) spectra of the HAs were recorded with a FTIR spectrometer (Bruker, Bremen, Germany). Briefly, the freeze-dried HAs were ground and homogenized with KBr, and then pressed into thin sheets [31]. The FTIR spectra of the thin sheets were scanned over the range of 500-4,000 cm^{-1} at a 2 cm^{-1} resolution. EEM spectra were collected using a Hitachi model F-7000 FL spectrophotometer (Tokyo, Japan). The slit widths of the excitation and emission spectra were set to 5 nm. The Em and Ex wavelengths were from 250 to 500 nm and from 200 to 450 nm, respectively. The interval was 5 nm with a scan speed of 2,400 nm/min [32]. The EEM spectra of distilled water were determined as a background solution before scanning the samples. And then, the EEM data of the distilled water was subtracted from each EEM spectra of the HA samples [33]. The first- and second-order Rayleigh and Raman scatters were also removed according to the protocol of Bahram et al. [34] to produce corrected EEM spectra.

2.5 PARAFAC analysis

The EEM spectral data were analysed using the PARAFAC method with the MATLAB 13.0 DOMFluor toolbox (MathWorks, Natick, MA, USA) [32]. A PARAFAC analysis was used to decompose the EEM spectral array into score, Ex loading, and Em loading matrices based on the trilinear decomposition theory [35]. The concentrations of the HAs as fluorescence components were evaluated with Fmax values from the score matrix [32].

2.6 Binding parameters

Eleven different concentrations of Cd(II) and Zn(II) were titrated into three HAs to evaluate the binding parameters. The modified Stern-Volmer equation [36,37] is a useful tool to estimate the binding parameters as follows:

$$\frac{F_0}{F_0 - F} = \frac{1}{f K_M C_M} + \frac{1}{f}$$

F_0 is the initial fluorescence intensity of the Fmax value without added metals; F is the fluorescence intensity at the Cd(II) and Zn(II) concentration, C_M ; and f represents the fraction of the initial fluorescence that corresponds to the binding fluorophores.

3 Results and discussion

3.1 Characterization of HAs

3.1.1 Elemental analysis of HAs

The elemental composition and atomic ratio are widely applied to study the nature of HAs [38]. The elemental composition and atomic ratio of the KW, PM, and GW-derived HAs is shown in Table 2. PM-derived HAs had the highest C content and the lowest O content, indicating a lower degree of oxidation [39]. The H/C atomic ratio indicates the aromatization of HAs, particularly aromatization conjugated with aliphatic chains [30,39]. In this study, the H/C ratios of the PM- and GW-derived HAs were similar, but a slightly higher H/C ratio was observed for the KW-derived HAs, suggesting a higher content of aromatic groups [40]. The sequences of the O/C and O/H atomic ratios of the HAs were in the order of GW > KW > PM. As the O/C atomic ratio is related to the content of COOH groups and COOH + OH groups [39], the content of COOH groups and COOH + OH groups of the HAs may be significantly different. To sum up, the diversity of the element content showed different degrees of oxidation and remarkable variations of HA functional groups, which may result in different binding effects to heavy metals.

3.1.2 FTIR analysis of HAs

FTIR spectroscopy is a feasible method to identify the functional groups of HAs derived from composts [41,42].

Table 2: Elemental analysis of HAs extracted from KW, PM and GW.

HAs	N	C	H	S	O	H/C	O/C	O/H	C/N
			Wt. %				Atom %		
KW-HA	1.32±0.03	50.36±0.29	7.05±0.08	0.08±0.01	41.19±0.34	1.68±0.02	0.61±0.01	0.37±0.01	44.52±0.68
PM-HA	4.95±0.18	57.98±0.43	7.33±0.08	2.80±0.05	26.94±0.22	1.52±0.03	0.35±0.01	0.23±0.00	13.68±0.61
GW-HA	3.44±0.08	49.28±0.10	6.22±0.08	0.25±0.01	40.81±0.05	1.51±0.02	0.62±0.00	0.41±0.01	16.72±0.42

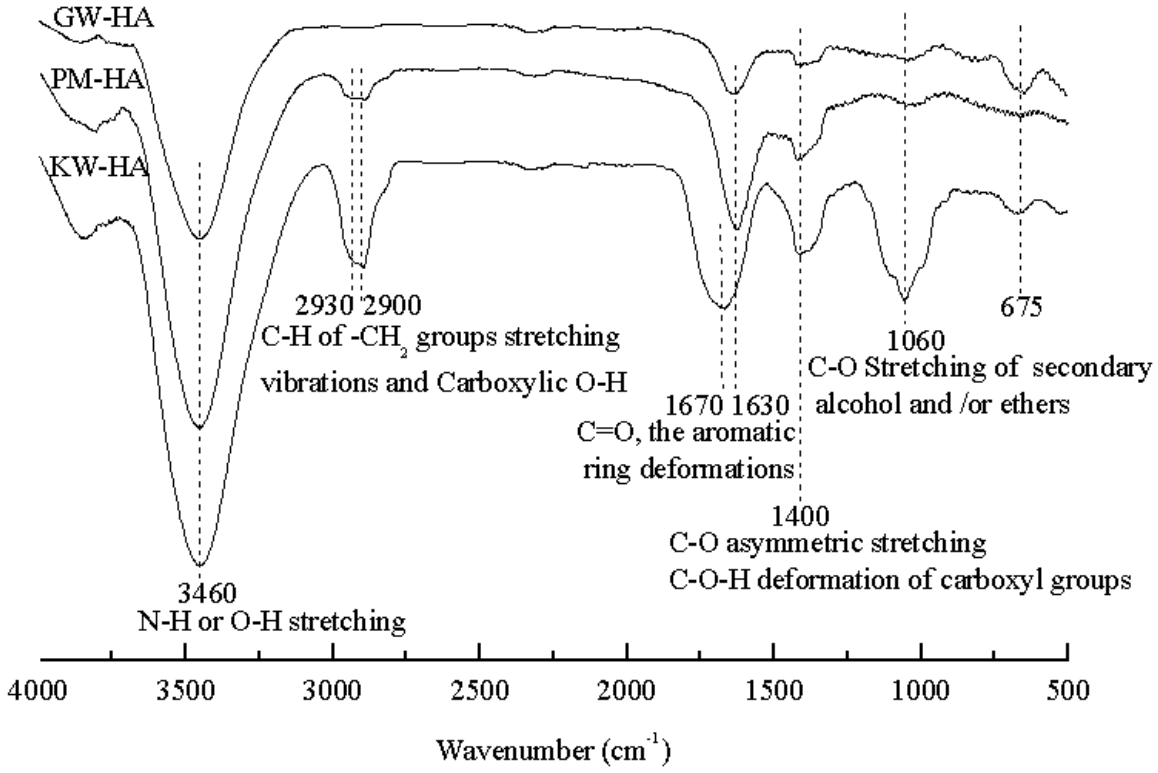

Figure 1: Fourier transform-infrared spectra of HAs extracted from KW, PM and GW.

The characteristic absorption bands of all samples are shown in Figure 1. The spectral shapes of the KW-, PM-, and GW-derived HAs were almost similar, except for the bands around 2,900 cm^{-1} which were attributed to C–H of $-CH_2$ groups stretching vibrations caused by amide hydrogen or OH groups of alcohols, phenols, organic acids and bands around 1,060 cm^{-1} which were interpreted to be C–O stretching of secondary alcohol and/or ethers [43] were obviously different. In addition, the absorbance intensity of particular peaks was more or less different. Absorbance intensity can be used to reveal the relative content of functional groups [43]. There were almost no significant absorption peaks for GW-derived HAs around 2,900 cm^{-1}, and very weak absorption peaks around 1,630 cm^{-1}, 1,400 cm^{-1} and 1,060 cm^{-1}. The relative content of functional groups can affect the binding ability of HAs and heavy metals, resulting in different fluorescence quenching effects of the KW-, PM-, and GW-derived HAs on the same heavy metals, which will be discussed later.

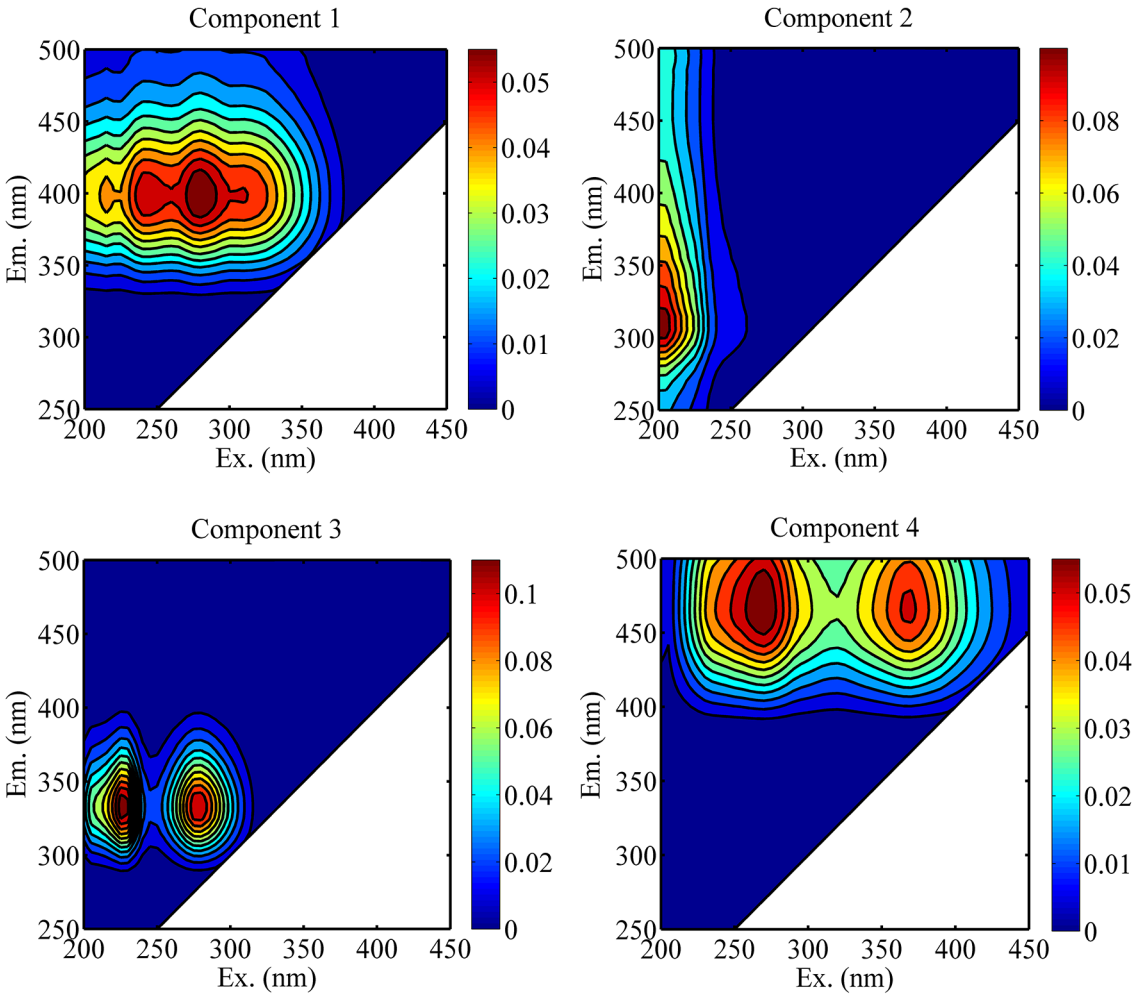

Figure 2: Four components of the three HAs identified by the PARAFAC analysis.

3.1.3 EEM-PARAFAC analysis of HAs

EEM spectroscopy is a useful tool to determine the composition of HAs, especially when combined with a PARAFAC analysis. As shown in Figure 2, four independent components were characterized by the EEM spectra and PARAFAC analysis in the three types of HAs. The peaks expressed as excitation/emission (Ex/Em) appeared as component 1 (C1, 235, 282/395 nm), component 2 (C2, 205/310 nm), component 3 (C3, 225, 280/335 nm), and component 4 (C4, 270, 368/475 nm), respectively. According to previous studies [25,41], C1 is associated with humic- and fulvic-like substances, C4 was identified as humic-like substances, and C2 and C3 were attributed to protein-like substances. Specifically, C2 was related to aromatic proteins and some of the tyrosine-like substances, and C3 was considered as tryptophan-like substances.

Simpler structural components bring about shorter wavelengths, whereas complex structural components cause relatively longer wavelengths [9,44]. Therefore, the complexity of the HA components was in the order of: C4 > C1 > C3 > C2. The Fmax values of the four components are shown in Figure 3. The C1, C2, C3, and C4 contents were significantly different, as they were derived from different raw materials. Similar results were also reported during the study of composting-derived fulvic acids [9]. The percentages of C1 and C4 of the KW-, PM-, GW-derived HAs were in the order of: PM > GW > KW, and the percentages of C2 and C3 were the highest in KW-derived HAs, suggesting higher condensation and polymerization with the PM- and GW-derived HAs than with the KW-derived HAs. Protein-like matter could be continuously converted into HAs during composting [25,45], thus, C2 and C3 in this study might be transformed into C1 and C4 if the composting

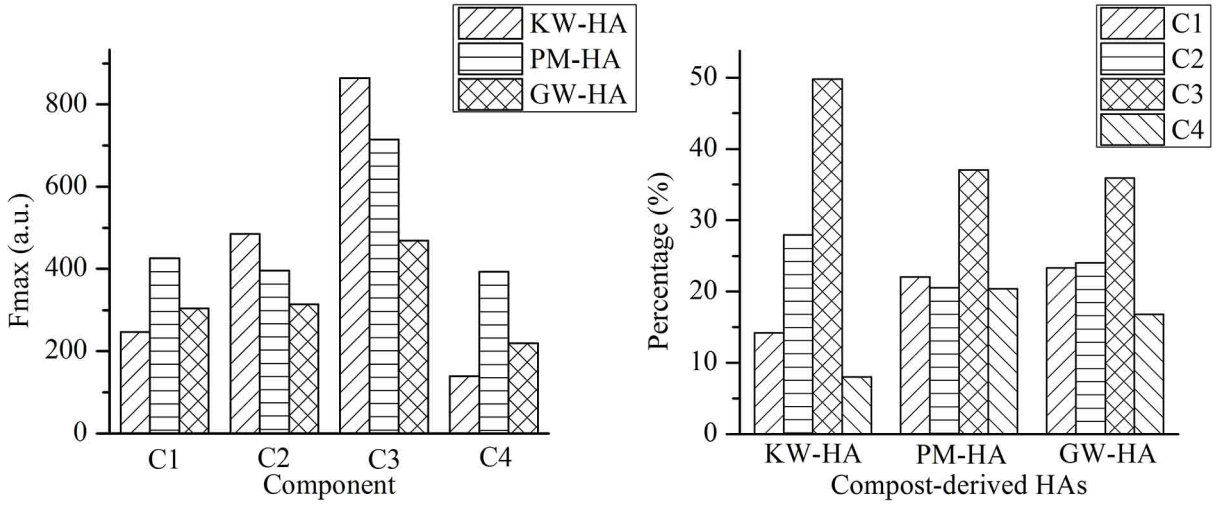

Figure 3: Fmax values of the four PARAFAC-derived components in three HAs without adding heavy metals and each component corresponding percentage in three Has.

time was much longer. However, this idea needs further research.

3.2 Binding behaviour of compost-derived HAs on Cd(II) and Zn(II)

3.2.1 EEM spectra of HAs titrated with Cd(II) and Zn(II)

Figure 4 shows the EEM spectra of the three HAs with or without titration of Cd(II) and Zn(II) at a total concentration of 100 μmol L^{-1}. As HAs include fulvic-like substances, humic-like substances, and protein-like matter, their EEM spectra were divided into five regions according to a previous study [46]. The results revealed that the EEM contours of the three HAs were different. Fluorescence quenching was relatively obvious with the increase in Cd**(II)** concentration but was slight with the increase in Zn**(II)** concentration, demonstrating that the decrease in fluorescence intensity was affected by the metal species. Similar results have been reported previously. Huang et al. [31] discovered the distinct complexation ability of copper and cadmium with the same DOM. He et al. [25] revealed a similar appearance between copper and lead binding with the same WEOM. All of these results may due to the differences in the ability of metal ions to accept electrons. The peak fluorescence spectrum almost appeared in region IV except that PM-derived HA were in region V, demonstrating that protein-like substances are a dominant component in KW and GW HAs which may be caused by immature compost. Interestingly, region IV always showed fluorescence quenching, regardless of whether Cd**(II)** or Zn**(II)** was added, indicating that protein-like substances are an important factor affecting mobilization of heavy metals.

3.2.2 The Fmax value curves of the HAs titrated with Cd(II) and Zn(II)

The Fmax curves of the PARAFAC-derived components were studied to further understand the quenching effects of Cd**(II)** and Zn**(II)** on HAs (Figure 5). Eleven different concentrations of Cd**(II)** and Zn**(II)** were titrated into three HAs. The results showed that the quenching effects were affected by the metal species and the HA source. Humic- and fulvic-like component C1 and humic-like component C4 revealed fluorescence quenching with the addition of Cd(II) in the KW- and PM-derived HAs, and the fluorescence quenching effect of PM-derived HAs was relatively stronger than that of KW-derived HAs, whereas negligible fluorescence quenching was detected in GW-derived HAs. Component C3 of all three HAs, representing tryptophan-like substances, showed larger fluctuations in fluorescence quenching curves with the increase in Cd**(II)** concentration, compared to components C1 and C4. Adding Zn(II) only caused fluorescence quenching of component C3 in all three HAs, but no significant change was observed in components C1 and C4. In a previous study, fulvic-like substances from municipal solid waste leachate strongly interacted with Cd(II) and Zn(II), however, the humic-like substances did not strongly combine with Cd(II) or Zn(II) [35]. The results of this research are only partially identical to the previous

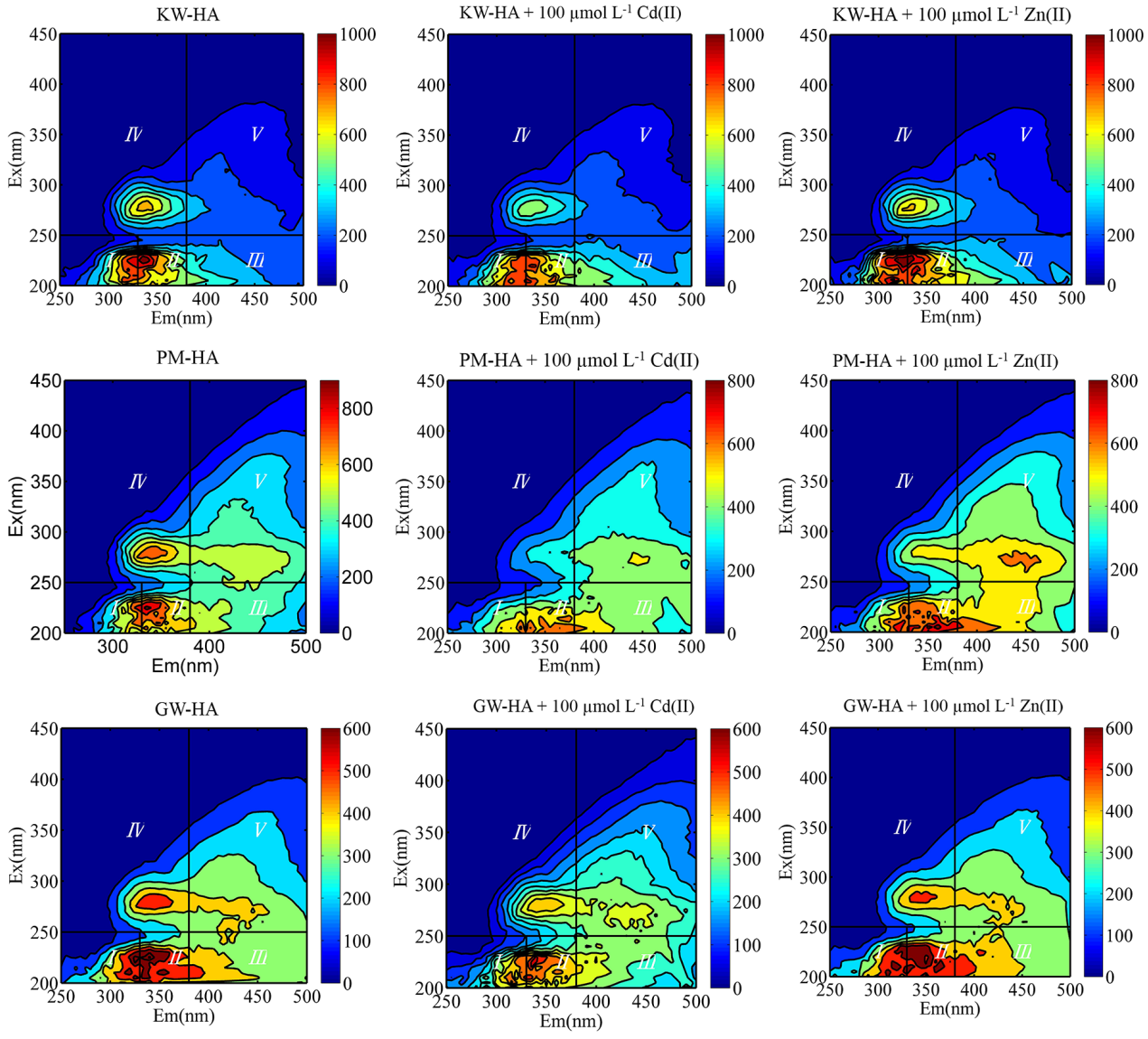

Figure 4: EEM spectra of the three HAs with or without titration of Cd(II) and Zn(II) at a total concentration of 100 μmol/L.

study, showing not only that the fulvic- and humic-like components C1 can combine with Cd(II), but also that the humic-like component C4 can also slightly combine with Cd(II) in the KW- and PM-derived HAs. In addition, the curve for component C2 increased for all HAs in the presence of Cd(II) and Zn(II). This result is similar to that of Wu et al. [35] who studied the interactions between DOM and Cd (II), Zn(II).

As mentioned above, the decline in the C1, C3, and C4 curves from the KW- and PM-derived HAs, and the decline in the C3 curve from GW-derived HAs could be attributed to Cd (II)-binding sites in fulvic-, humic-like substances as well as protein-like matter. According to a previous study [47], the binding sites around 3,427 cm^{-1} and 1,599 cm^{-1} of the FTIR spectra played an important role in the HA-metal binding process. To our knowledge, bands around 3,427 cm^{-1} have been interpreted to be N–H or OH stretching vibrations, which may be caused by amide hydrogen or OH groups of alcohols, phenols, and organic acids. Bands around 1,599 cm^{-1} are mainly associated with the C=O, the aromatic ring deformations, bonded conjugated ketones and CO in quinones and amides [41-43,48]. In this study, the intensity peaks around 3,427 cm^{-1} and 1,599 cm^{-1} could be lower in the GW-derived HAs than that of KW- and PM-derived HAs, which may lead to the negligible fluorescence quenching. In addition, the peak at 2,924

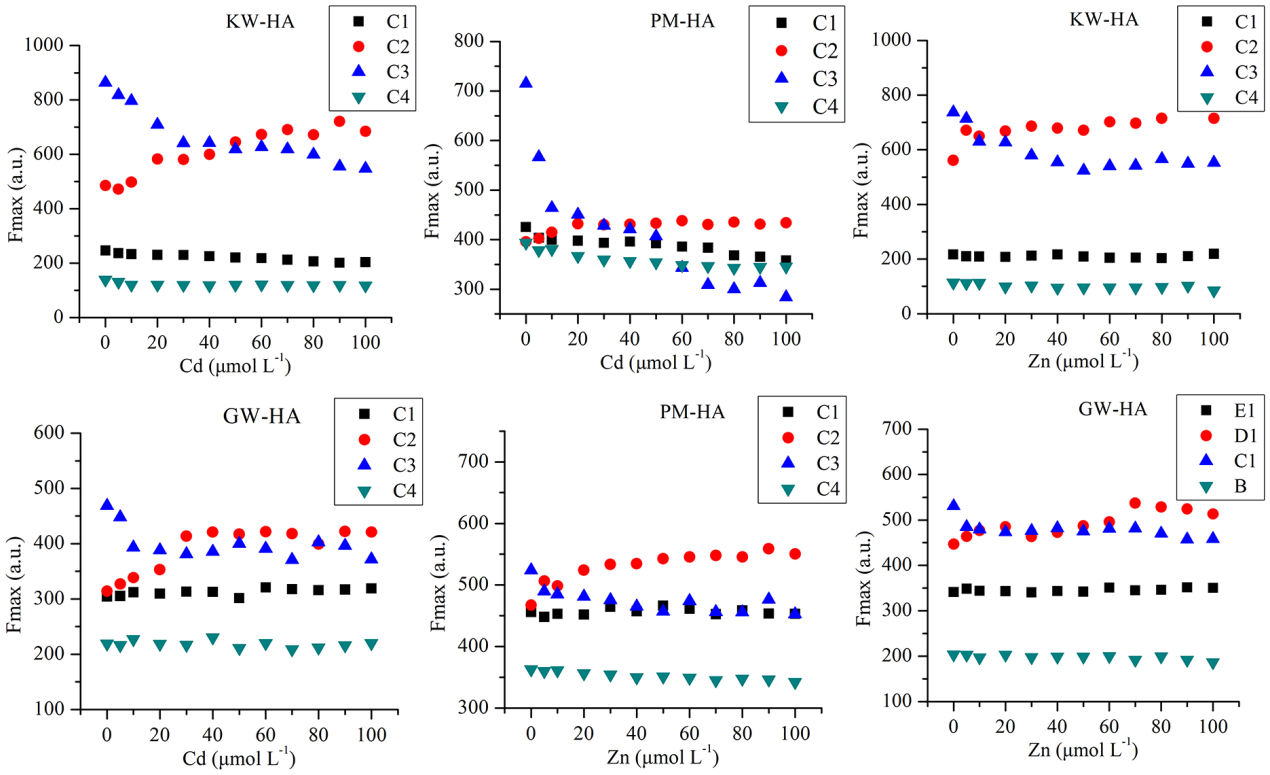

Figure 5: Changes in the Fmax values of the four PARAFAC-derived components after titrating Cd(II) and Zn(II).

cm^{-1} and 2,853 cm^{-1} was still involved in the HA-metal binding process [47], but we could not see the peak clearly in the GW HAs.

The rapid decline in the C3 curves of all HAs is worth noting. The larger fluctuations in fluorescence quenching curves are likely due to the Cd(II) and Zn(II) complexation of protein-like components. A similar phenomenon was reported previously [24,31]. These findings suggest that C3 influences the affinity behaviour of compost-derived HAs on metals, which is consistent with the fluorescence spectra described above. As C3 is protein-like matter, it may be converted to more stable substances, such as HAs over time, and it may be impossible to complex more heavy metals as originally shown. Furthermore, the upward curves of C2 components were attributed to the changes in quantum yields of protein fluorescence with the addition of Cd(II) and Zn (II), or that the fluorescence of the protein-like components might have been quenched with other components before adding Cd(II) and Zn (II), whereas, the occurred of Cd(II) and Zn (II) replaced the original quencher, and finally, the fluorescence intensity was enhanced [49]. A similar phenomenon was discovered in the work of Huang et al. [31]. Another explanation is that protein-like substances are enhanced or quenched by unpredictably binding with heavy metals. Although many studies have used the EEM-PARAFAC method to evaluate the ability of HAs to bind to heavy metals, some researchers have reported that the method may not be appropriate, as the stability of the complex derived from protein-like substances and metals may cause unpredictable changes in the curves [35]. However, in this study, protein-like substances C2 and C3 showed consistent changes such that component C2 was always upward and component C3 was always downward.

3.3 Metal binding parameters

Metal binding parameters were employed through the modified Stern-Volmer equation to evaluate the binding ability of the compost-derived HAs on Cd(II) (Table 3). The log K_m values of the fulvic- and humic-like fractions C1 and humic-like fractions C4 ranged from 4.21 to 4.81 and from 4.89 to 5.09 respectively, and those of the protein-like fractions ranged from 4.33 to 5.06. These results are similar to other studies [36,47]. Among all components, component C1 showed a relatively lower log K_m than component C4, suggesting that the affinities between Cd(II) and the C4 components were much stronger. This result may be attributed to the phenolic and aromatic

Table 3 Binding parameters between Cd(II) and components derived from three HAs calculated by the modified Stern-Volmer equation

HAs	fraction	logKm	R^2
	KW-C1	4.81	0.923
KW-HA	KW-C3	4.33	0.971
	KW-C4	5.09	0.949
	PM-C1	4.21	0.901
PM-HA	PM-C3	5.06	0.918
	PM-C4	4.89	0.969
GW-HA	GW-C3	4.65	0.921

carboxylic groups in the humic-like fractions, which can combine with metals in stable ring structures [36]. In addition, the binding values could not be modelled well in the KW-, PM- and GW-HAs for Zn(II), even though similar quenching curves were observed in protein-like fractions, suggesting a different binding mechanism between Zn(II) and the KW-, PM- and GW-HAs [35].

4 Conclusions

This study has given an account of the structure and fractions of three HAs and their binding processes with Cd(II) and Zn(II). The results suggest that although the three HAs had similar functional groups and elemental composition, their content and fractions were different, thus, their metal binding capacities were different. The EEM-PARAFAC analysis successfully provided an additional interpretation about their binding properties, which have been demonstrated to be affected by metal species and raw materials. In summary, the KW- and PM-derived HAs gave the fastest responses after adding Cd (II). The ability of HAs to bind with Cd (II) was stronger than that of Zn (II) for all three HAs. The PM- and KW-derived HAs may be a better choice for binding with heavy metals than the GW-derived HAs. Taken together, the results of this study will be essential for predicting the environmental behaviour of heavy metals in compost applied farmland soils. The protein-like components, humic- and fulvic-like components in composts may be important indicators for controlling the migration and transformation of heavy metals in farmland soils. However, the HAs in this study were only characterized as groups, the characterization and metal binding behaviours of those HAs at specific molecular level remain unknown. Moreover the stability of the complexes derived from protein-like, humic- and fulvic- like substances and metals in farmland soils also requires further research.

Acknowledgements: This study was supported by the GDAS' Project of Science and Technology Development (2019GDASYL-0501005), the Program of Guangdong Provincial Key Laboratory of New and Renewable Energy Research and Development, China (y809jm1001) and the Science and Technology Planning Project of Guangzhou City (No. 201903010071)

References

[1] Zhang L, Sun X. Addition of seaweed and bentonite accelerates the two-stage composting of green waste. Bioresour Technol. 2017 Nov;243:154–62.
[2] Wu S, Shen Z, Yang C, Zhou Y, Li X, Zeng G, et al. Effects of C/N ratio and bulking agent on speciation of Zn and Cu and enzymatic activity during pig manure composting. Int Biodeterior Biodegradation. 2017 Apr;119:429–36.
[3] Wang X, Zhang W, Gu J, Gao H, Qin Q. Effects of different bulking agents on the maturity, enzymatic activity, and microbial community functional diversity of kitchen waste compost. Environ Technol. 2016 Oct;37(20):2555–63.
[4] Wang H, Xu J, Sheng L. Study on the comprehensive utilization of city kitchen waste as a resource in China. Energy. 2019 Apr;173:263–77.
[5] Dhyani V, Kumar Awasthi M, Wang Q, Kumar J, Ren X, Zhao J, et al. Effect of composting on the thermal decomposition behavior and kinetic parameters of pig manure-derived solid waste. Bioresour Technol. 2018 Mar;252:59–65.
[6] Pedrazzi S, Santunione G, Minarelli A, Allesina G. Energy and biochar co-production from municipal green waste gasification: A model applied to a landfill in the north of Italy. Energy Convers Manage. 2019 May;187:274–82.
[7] Awasthi MK, Wang Q, Huang H, Li R, Shen F, Lahori AH, et al. Effect of biochar amendment on greenhouse gas emission and bio-availability of heavy metals during sewage sludge co-composting. J Clean Prod. 2016 Nov;135:829–35.
[8] Wu J, Zhao Y, Qi H, Zhao X, Yang T, Du Y, et al. Identifying the key factors that affect the formation of humic substance during different materials composting. Bioresour Technol. 2017 Nov;244(Pt 1):1193–6.
[9] Zhao Y, Wei Y, Zhang Y, Wen X, Xi B, Zhao X, et al. Roles of composts in soil based on the assessment of humification degree of fulvic acids. Ecol Indic. 2017 Jan;72:473–80.
[10] Li F, Zhang J, Liu W, Liu J, Huang J, Zeng G. An exploration of an integrated stochastic-fuzzy pollution assessment for heavy metals in urban topsoil based on metal enrichment and bioaccessibility. Sci Total Environ. 2018 Dec;644:649–60.
[11] Li F, Zhang J, Jiang W, Liu C, Zhang Z, Zhang C, et al. Spatial health risk assessment and hierarchical risk management for mercury in soils from a typical contaminated site, China. Environ Geochem Health. 2017 Aug;39(4):923–34.
[12] Wu J, Zhao Y, Zhao W, Yang T, Zhang X, Xie X, et al. Effect of precursors combined with bacteria communities on the

formation of humic substances during different materials composting. Bioresour Technol. 2017 Feb;226:191–9.
[13] Li S, Li D, Li J, Li G, Zhang B. Evaluation of humic substances during co-composting of sewage sludge and corn stalk under different aeration rates. Bioresour Technol. 2017 Dec;245(Pt A):1299-302. https://doi.org/10.1016/j.biortech.2017.08.177.
[14] Wang C, Tu Q, Dong D, Strong PJ, Wang H, Sun B, et al. Spectroscopic evidence for biochar amendment promoting humic acid synthesis and intensifying humification during composting. J Hazard Mater. 2014 Sep;280:409–16.
[15] Vialykh EA, Ilarionov SA, Zhdanova AV. Amino acid composition analysis of humic acids isolated by sequential alkaline extraction from soil, In: Xu J, Wu J, He Y, editors. Functions of natural organic matter in changing environment. The 16th Meeting of the International Humic Substances Society; 2012 Sep 9-14; Hangzhou, China. Berlin: Springer; 2013. p. 215-18. https://doi.org/10.1007/978-94-007-5634-2_38.
[16] Boguta P, D'Orazio V, Senesi N, Sokołowska Z, Szewczuk-Karpisz K. Insight into the interaction mechanism of iron ions with soil humic acids. The effect of the pH and chemical properties of humic acids. J Environ Manage. 2019 Sep;245:367–74.
[17] Phong DD, Hur J. Using two-dimensional correlation size exclusion chromatography (2D-CoSEC) and EEM-PARAFAC to explore the heterogeneous adsorption behavior of humic substances on nanoparticles with respect to molecular sizes. Environ Sci Technol. 2018 Jan;52(2):427–35.
[18] Morais Camilo LM, Lima Kassio MG. Comparing unfolded and two-dimensional discriminant analysis and support vector machines for classification of EEM data. Chemom Intell Lab Syst. 2017;170:1–12.
[19] Yu GH, He PJ, Shao LM. Novel insights into sludge dewaterability by fluorescence excitation-emission matrix combined with parallel factor analysis. Water Res. 2010 Feb;44(3):797–806.
[20] He XS, Xi BD, Li D, Guo XJ, Cui DY, Pan HW, et al. Influence of the composition and removal characteristics of organic matter on heavy metal distribution in compost leachates. Environ Sci Pollut Res Int. 2014 Jun;21(12):7522–9.
[21] Wu J, Zhang H, Yao QS, Shao LM, He PJ. Toward understanding the role of individual fluorescent components in DOM-metal binding. J Hazard Mater. 2012 May;215-216:294–301.
[22] Wu J, Zhang H, Shao LM, He PJ. Fluorescent characteristics and metal binding properties of individual molecular weight fractions in municipal solid waste leachate. Environ Pollut. 2012 Mar;162:63–71.
[23] He XS, Xi BD, Cui DY, Liu Y, Tan WB, Pan HW, et al. Influence of chemical and structural evolution of dissolved organic matter on electron transfer capacity during composting. J Hazard Mater. 2014 Mar;268:256–63.
[24] Yuan DH, Guo XJ, Wen L, He LS, Wang JG, Li JQ. Detection of Copper (II) and Cadmium (II) binding to dissolved organic matter from macrophyte decomposition by fluorescence excitation-emission matrix spectra combined with parallel factor analysis. Environ Pollut. 2015 Sep;204:152–60.
[25] He XS, Xi BD, Pan HW, Li X, Li D, Cui DY, et al. Characterizing the heavy metal-complexing potential of fluorescent water-extractable organic matter from composted municipal solid wastes using fluorescence excitation–emission matrix spectra coupled with parallel factor analysis. Environ Sci Pollut Res Int. 2014;21(13):7973–84.
[26] Ding Y, Liu M, Peng S, Li J, Liang Y, Shi Z. Binding characteristics of heavy metals to humic acid before and after fractionation by ferrihydrite. Chemosphere. 2019 Jul;226:140–8.
[27] Wu G, Kang H, Zhang X, Shao H, Chu L, Ruan C. A critical review on the bio-removal of hazardous heavy metals from contaminated soils: issues, progress, eco-environmental concerns and opportunities. J Hazard Mater. 2010 Feb;174(1-3):1–8.
[28] Peng W, Li X, Song J, Jiang W, Liu Y, Fan W. Bioremediation of cadmium- and zinc-contaminated soil using Rhodobacter sphaeroides. Chemosphere. 2018 Apr;197:33–41.
[29] Zhang C, Katayama A. Humin as an electron mediator for microbial reductive dehalogenation. Environ Sci Technol. 2012 Jun;46(12):6575–83.
[30] Aranganathan L, Radhika Rajasree SR, Suman TY, Remya RR, Gayathri S, Jayaseelan C, et al. Comparison of molecular characteristics of Type A humic acids derived from fish waste and sugarcane bagasse co-compost influenced by various alkaline extraction protocols. Microchem J. 2019 Sep;149:104038.
[31] Huang M, Li Z, Huang B, Luo N, Zhang Q, Zhai X, et al. Investigating binding characteristics of cadmium and copper to DOM derived from compost and rice straw using EEM-PARAFAC combined with two-dimensional FTIR correlation analyses. J Hazard Mater. 2018 Feb;344:539–48.
[32] Yu Z, Liu X, Zhao M, Zhao W, Liu J, Tang J, et al. Hyperthermophilic composting accelerates the humification process of sewage sludge: molecular characterization of dissolved organic matter using EEM-PARAFAC and two-dimensional correlation spectroscopy. Bioresour Technol. 2019 Feb;274:198–206.
[33] Lawaetz AJ, Stedmon CA. Fluorescence intensity calibration using the Raman scatter peak of water. Appl Spectrosc. 2009 Aug;63(8):936–40.
[34] Bahram M, Bro R, Stedmon CA, Afkhami A. Handling of Rayleigh and Raman scatter for PARAFAC modeling of fluorescence data using interpolation. J Chemometr. 2006 Mar;20(3-4):99–105.
[35] Wu J, Zhang H, He PJ, Shao LM. Insight into the heavy metal binding potential of dissolved organic matter in MSW leachate using EEM quenching combined with PARAFAC analysis. Water Res. 2011 Feb;45(4):1711–9.
[36] Chen W, Habibul N, Liu XY, Sheng GP, Yu HQ. FTIR and synchronous fluorescence heterospectral two-dimensional correlation analyses on the binding characteristics of copper onto dissolved organic matter. Environ Sci Technol. 2015 Feb;49(4):2052–8.
[37] Berkovic AM, García Einschlag FS, Gonzalez MC, Pis Diez R, Mártire DO. Evaluation of the Hg2+ binding potential of fulvic acids from fluorescence excitation-emission matrices. Photochem Photobiol Sci. 2013 Feb;12(2):384–92.
[38] Chefetz B, Adani F, Genevini P, Tambone F, Hadar Y, Chen Y. Humic-Acid transformation during composting of municipal solid waste. J Environ Qual. 1998;27(4):794–800.
[39] Eneji AE, Honna T, Yamamoto S, Masuda T, Endo T, Irshad MA. Changes in humic substances and phosphorus fractions during composting. Commun Soil Sci Plant Anal. 2003 Aug;34(15-16):2303–14.

[40] Veeken A, Nierop K, Wilde VD, Hamelers B. Characterisation of NaOH-extracted humic acids during composting of a biowaste. Bioresour Technol. 2000 Mar;72(1):33–41.
[41] Yuan Y, Xi B, He X, Tan W, Gao R, Zhang H, et al. Compost-derived humic acids as regulators for reductive degradation of nitrobenzene. J Hazard Mater. 2017 Oct;339:378–84.
[42] Asses N, Farhat A, Cherif S, Hamdi M, Bouallagui H. Comparative study of sewage sludge co-composting with olive mill wastes or green residues: process monitoring and agriculture value of the resulting composts. Process Saf Environ Prot. 2018 Feb;114:25–35.
[43] Wang Q, Awasthi MK, Zhao J, Ren X, Li R, Wang Z, et al. Improvement of pig manure compost lignocellulose degradation, organic matter humification and compost quality with medical stone. Bioresour Technol. 2017 Nov;243:771–7.
[44] Wei Z, Xi B, Zhao Y, Wang S, Liu H, Jiang Y. Effect of inoculating microbes in municipal solid waste composting on characteristics of humic acid. Chemosphere. 2007 Jun;68(2):368–74.
[45] Tuomela M, Vikman M, Hatakka A, Itävaara M. Biodegradation of lignin in a compost environment: a review. Bioresour Technol. 2000 Apr;72(2):169–83.
[46] Chen W, Westerhoff P, Leenheer JA, Booksh K. Fluorescence excitation-emission matrix regional integration to quantify spectra for dissolved organic matter. Environ Sci Technol. 2003 Dec;37(24):5701–10.
[47] Shi W, Lü C, He J, En H, Gao M, Zhao B, et al. Nature differences of humic acids fractions induced by extracted sequence as explanatory factors for binding characteristics of heavy metals. Ecotoxicol Environ Saf. 2018 Jun;154:59–68.
[48] Kaal J, Cortizas AM, Biester H. Downstream changes in molecular composition of DOM along a headwater stream in the Harz mountains (Central Germany) as determined by FTIR, Pyrolysis-GC-MS and THM-GC-MS. J Anal Appl Pyrolysis. 2017 Jul;126:50–61.
[49] Yamashita Y, Jaffé R. Characterizing the interactions between trace metals and dissolved organic matter using excitation-emission matrix and parallel factor analysis. Environ Sci Technol. 2008 Oct;42(19):7374–9.